Journal of Nuclear Materials 392 (2009) 95–99

Contents lists available at ScienceDirect

Journal of Nuclear Materials

journal homepage: www.elsevier.com/locate/jnucmat

Solubility of ThO_2 in $Gd_2Zr_2O_7$ pyrochlore: XRD, SEM and Raman spectroscopic studies

B.P. Mandal [a], Nandini Garg [b], S.M. Sharma [b], A.K. Tyagi [a,*]

[a] Chemistry Division, Bhabha Atomic Research Centre, Mumbai 400 085, India
[b] High Pressure Physics Division, Bhabha Atomic Research Centre, Mumbai 400 085, India

ARTICLE INFO

Article history:
Received 24 November 2008
Accepted 23 March 2009

ABSTRACT

Solubility of ThO_2 in gadolinium zirconate pyrochlore, a potential host for radioactive materials, has been investigated. The phase relations in $Gd_{2-x}Th_xZr_2O_{7+x/2}$ ($0.0 \leq x \leq 2.0$) systems have been established under the slow-cooled conditions from 1400 °C. XRD studies reveal that the compositions corresponding to $x = 0.0$–0.075 are single phasic in nature and beyond $x \geq 0.1$ the biphasic region starts. The first biphasic region comprising of pyrochlore and thoria exist from $x = 0.1$–0.8, and from $x = 1.2$ another biphasic region consisting of gadolinia stabilized zirconia (GSZ) and thoria appears which persists till $x = 1.6$. The end member (i.e. $x = 2.0$) of the series is found to be a mixture of monoclinic ZrO_2 and thoria. Interestingly, gadolinia which has wide solubility in thoria, did not show any miscibility in thoria in the presence of zirconia. Irregular grains of $Gd_{1.8}Th_{0.2}Zr_2O_{7.1}$ as shown in SEM supports its biphasic nature. Raman spectra of heavily thoria doped ($x = 0.1$ and 0.2) samples, indicates the presence of $Zr–O_7$ mode which implies the samples are highly disordered in nature.

1. Introduction

With the development of advanced and newer generation reactors, the problem of safe disposal of the nuclear waste has become more challenging and a lot of attention needs to be paid to develop newer and safer technologies [1]. In the interest of public acceptance and the safety, several groups are involved in search for a suitable matrix for the safe disposal of the nuclear wastes [2,3]. A number of materials (like glasses, ceramics etc.) are being considered for this purpose. Borosilicate glass has a tendency to get devitrified in the presence of water and steam at elevated pressure and temperature, e.g. 300–400 °C and 300–1000 bar [2]. The lower end of this pressure–temperature range may be encountered by glass cylinder after burial in geological repositories. Furthermore, prevention of water ingression to the radwaste is extremely difficult which may form water soluble salt and increase the leachability of certain species [3]. For the fixation of actinides, the ceramic matrix has several advantages viz. higher thermodynamic stability, lower leachability, higher chemical and radiation stability [4]. The thermal expansion coefficient should not be very high but the thermal conductivity should be high enough [1–8].

Pyrochlores are contemplated to be important host materials for nuclear waste incorporation [9–11]. Pyrochlores have the general formula $A_2B_2O_7$ where A is the larger cation and B is the smaller one. In most of the cases A is a trivalent rare-earth ion, but can also be a mono or divalent cation, and B may be 3d, 4d or 5d transition element having an appropriate oxidation state required for charge balance to give rise to the composition $A_2B_2O_7$. The space group of the ideal pyrochlore is $Fd\bar{3}\,m$ [12]. The pyrochlore structure is reported [13,14] as a network consisting of corner linked of BO_6 octahedra with A atoms filling the interstices. All the oxygen atoms are not equivalent in pyrochlore structure. The oxygen at 48*f* position is surrounded by two A and two B cations whereas the oxygen at 8*b* position is surrounded by four A cations. The 8*a* position which remains vacant is surrounded by four B cations. Pyrochlores are step forward in the development of oxide compounds for IMF applications because the pyrochlore crystal structure permits a wide range of substitutions from the rare-earth elements [15,16]. Besides the ability of fixation of actinides, pyrochlores are having lot of use in piezoelectric, dielectric, semiconductors, etc. [12,17,18]. Defect pyrochlores can be used as solid electrolyte due to their excellent ionic conductivity [19]. In view of these wide ranging applications, theoreticians have also been showing considerable interest in investigation of structure and properties of new pyrochlores [20].

Thoria is going to play an important role in futuristic nuclear technology and hence it will be essential to fix the ThO_2, minor actinides including americium, berkelium and other fission products in a common matrix [21]. Lian et al. showed the stability against radiation improves with increase in Fe_2O_3 and ThO_2 content in $Y_2Ti_2O_7$ systems [22]. It has been found that zirconate pyrochlores specially $Gd_2Zr_2O_7$ owing to lower r_A/r_B radius ratio, are extremely stable under high and low energy radiation environments

* Corresponding author. Tel.: +91 22 2559 5330; fax: +91 22 2550 5151.
E-mail address: aktyagi@barc.gov.in (A.K. Tyagi).

0022-3115/$ - see front matter © 2009 Elsevier B.V. All rights reserved.
doi:10.1016/j.jnucmat.2009.03.050

[23]. Hence we have chosen $Gd_2Zr_2O_7$ as a suitable host material for fixation of ThO_2. McCarthy et al. [2] investigated the solubility of Ce^{4+} in $Gd_2Zr_2O_7$ to simulate the solubility of Pu^{4+} in the pyrochlore matrix. To simulate the solubility of Am^{3+} in the above mentioned pyrochlore we have investigated the solubility of Nd^{3+} in $Gd_2Zr_2O_7$ [24]. Since Konings et al. have mentioned that thorium can be used as a surrogate for plutonium and americium [25] we expect to simulate the solubility of these ions by investigating the solubility of thorium in the pyrochlore matrix. There are several studies of the A and B site doping in $Gd_2Zr_2O_7$ pyrochlore by isovalent ions [24,26,27] and aliovalent ions [28]. However, the phase relation and structure of ThO_2 doped in $Gd_2Zr_2O_7$ pyrochlore still remains unexplored. In this manuscript, XRD, SEM and Raman spectroscopic studies have been exploited to delineate the solubility limit and observe the microstructure of ThO_2 in gadolinium zirconate pyrochlore.

2. Experimental details

To remove moisture and other volatile impurities AR grade Gd_2O_3, ZrO_2 and ThO_2 were first heated overnight at 900 °C. Stoichiometric amounts of the reactants were weighed to get the compositions corresponding to $Gd_{2-x}Th_xZr_2O_{7+x/2}$ $(0.0 \leq x \leq 2.0)$. The homogenized mixtures were then subjected to a three-step heating protocol as follows with intermittent grindings. The thoroughly ground mixtures were heated in the pellet form at 1200 °C for 36 h, followed by a second heating at 1300 °C for 36 h after regrinding and repelletizing. In order to attain a better homogeneity, the products obtained after second heating were reground, pelletized and heated at 1400 °C for 48 h, which was the final annealing temperature for all the specimens. The heating and cooling rates were 2 °C per minute in all the annealing steps and atmosphere was static air. The XRD pattern of the samples was recorded from $2\theta = 10$ to 90° on a Philips X'pert Pro XRD unit in static air condition with monochromatized Cu $K\alpha$ radiation ($K\alpha_1 = 1.5406$ Å and $K\alpha_2 = 1.5444$ Å).

The microstructure of the sintered pellets was investigated using a VEGA TS 5130 MM Scanning Electron Microscope (TESCAN, Brno, Czech Republic). The Raman spectra was recorded using an indigenously developed micro Raman system. In this instrument, a 20× objective is used with confocal optics and a CCD based single stage spectrograph along with a super notch filter. For the measurements presented here we used 532 nm line of solid state diode laser as the excitation source. The size of the laser spot was less than 10 μm.

3. Results and discussion

XRD of all the products in $Gd_{2-x}Th_xZr_2O_{7+x/2}$ $(0.0 \leq x \leq 2.0)$ series were recorded and analyzed and few representative XRD patterns are shown in Fig. 1. Pure $Gd_2Zr_2O_7$ crystallizes as pyrochlore which is evident by the presence of super-lattice peaks at $2\theta \approx 14°(1\,1\,1)$, $27°(3\,1\,1)$, $37°(3\,3\,1)$, $45°(5\,1\,1)$ (using Cu $K\alpha$ as radiation source) [19,24]. The Fig. 1(a)–(d) represent the XRD patterns of pyrochlore phase for the compositions corresponding to $x = 0.0$–0.075 whereas Fig. 1(e) exhibits the onsets of phase separation (fifth row in Table 1) to pyrochlore and thoria (marked by asterisks). The shifting of the diffraction peaks towards lower angle on doping (Fig. 1) clearly indicates the cell parameters of the doped pyrochlores increase as the concentration of Th^{4+} is increased. The cell parameters and cell volume of all the compositions were calculated using POWDERX program and it has been found that the cell parameter increases with increase in Th^{4+} content in the solid solution in the homogeneity range (Table 1). Since the ionic radii of Gd^{3+} and Th^{4+}, in 8-fold coordination, [29] are similar (0.98 Å), based on the relative ionic size considerations, one could

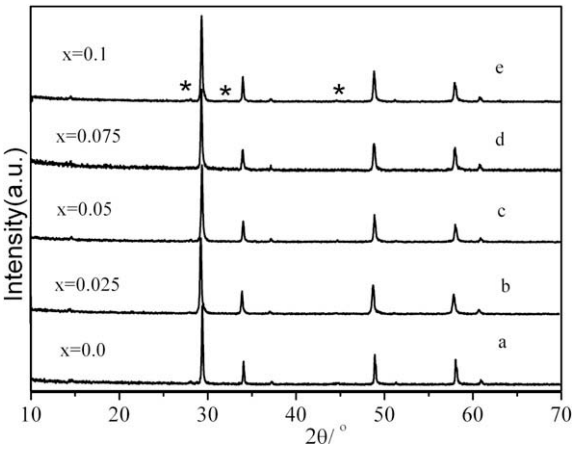

Fig. 1. Typical XRD patterns of $Gd_{2-x}Th_xZr_2O_{7+x/2}$ ((a) $x = 0.0$, (b) $x = 0.025$, (c) $x = 0.05$, (d) $x = 0.075$, and (e) $x = 0.1$) (asterisk shown in pattern of $x = 0.1$ indicates presence of F type phase of ThO_2 as secondary phase.)

expect that there should not be any increase in lattice parameter or cell volume upon substitution of Th^{4+} in $Gd_2Zr_2O_7$. Qu et al. [30] have shown that when $Sm_2Zr_2O_7$ was doped with MgO (concentration <7.5 mol%) it resulted in an increase of the lattice parameter of the solid solution, though the ionic radii of Mg^{2+} is smaller than that of Sm^{3+}. They have suggested that this increase in cell parameter is due to the repulsion among the dopants incorporated at the interstitial sites. In our study also it is possible that during the course of substitution of Gd^{3+} by Th^{4+} in the solid solution, the extra 1/2 oxygen enters into the lattice which may occupy the vacant 8*a* site or the interstitial sites resulting in an increase in the cell parameter due to mutual repulsion.

Interestingly, the whole biphasic region ($x = 0.1$–2.0) does not comprise of the same components (see Table 1). Fig. 2 depicts the typical XRD patterns of three different biphasic regions in the whole composition range. In first biphasic region i.e. $x = 0.1$–0.8, the intensity of the peaks of the secondary phase (F-type ThO_2) increases with increase in thoria concentration in the nominal compositions which implies that there is an increment of the content of the secondary phase in the biphasic mixture (Fig. 2(a) and (b)). The intensity of the peaks of the secondary phase (F-type ThO_2) is too small in the compositions $x = 0.1$ and 0.2 to make meaningful refinement. Therefore, asterisks have been used in Table 1 instead of any cell parameter. The peak marked with $ in inset of Fig. 2(a) is due to the unreacted monoclinic ZrO_2. In the second biphasic region, i.e. $x = 1.2$–1.6, in addition to F-type thoria phase, the diffraction peaks corresponding to cubic gadolinia stabilized zirconia (GSZ) are observed. These diffraction peaks look similar to that of the pyrochlores structure. However, when observed carefully we see that these diffraction patterns (Fig. 2(c) and (d)) do not have the characteristic superstructure diffraction peaks of the pyrochlore structure. Moreover, we also observe that as expected the most intense diffraction peak of the GSZ structure (29.6°) is at a higher two theta angle than that of the pyrochlores structure (29.3°). In the compositions $x = 1.2$–1.6, the peaks corresponding to cubic gadolinia stabilized zirconia (GSZ) appear at lower angle compared to pure cubic zirconia. Grover and Tyagi [31] showed that 20 mol% $GdO_{1.5}$ can stabilize cubic zirconia which supports our present study. The last compositions i.e. $Th_2Zr_2O_8$ ($Th_{0.5}Zr_{0.5}O_2$) is a mixture of monoclinic ZrO_2 and thoria (Fig. 2(e)) which indicates that no reaction takes place between the reactants at that thermodynamic condition.

Earlier it was found that 30 mol% $GdO_{1.5}$ can be dissolved in thoria [32]. In the compositions of second biphasic region i.e. $Gd_{0.8}Th_{1.2}Zr_2O_{7.6}$ and $Gd_{0.4}Th_{1.6}Zr_2O_{7.8}$ though both ZrO_2 and

Table 1
Phase analysis and lattice parameters of the phases $Gd_{2-x}Th_xZr_2O_{7+x/2}$ systems, annealed at 1400 °C followed by slow cooling.

Sr. No	Compositions	Phase identification	Lattice parameter (Å)	Volume (Å3)
1	$Gd_2Zr_2O_7$	P	10.528(3)	1167(5)
2	$Gd_{1.975}Th_{0.025}Zr_2O_{7.0125}$	P	10.540(1)	1170.9(1)
3	$Gd_{1.95}Th_{0.05}Zr_2O_{7.025}$	P	10.541(1)	1171(1)
4	$Gd_{1.925}Th_{0.075}Zr_2O_{7.0375}$	P	10.542(1)	1171(1)
5	$Gd_{1.9}Th_{0.1}Zr_2O_{7.05}$	P	a_P = 10.542(1)	1171(2)
		F	*	*
6	$Gd_{1.8}Th_{0.2}Zr_2O_{7.1}$	P	a_P = 10.542(2)	1171(3)
		F	*	*
7	$Gd_{1.6}Th_{0.4}Zr_2O_{7.2}$	P	a_P = 10.542(1)	1171(2)
		F	a_F = 5.584(3)	174.1(1)
8	$Gd_{1.2}Th_{0.8}Zr_2O_{7.4}$	P	a_P = 10.542(1)	1171(2)
		F	a_F = 5.584(3)	174.1(1)
9	$Gd_{0.8}Th_{1.2}Zr_2O_{7.6}$	F (ThO_2)	a_F = 5.584(2)	174.1(1)
		F′ (GSZ)	a'_F = 5.234(2)	143.5(1)
10	$Gd_{0.4}Th_{1.6}Zr_2O_{7.8}$	F (ThO_2)	a'_F = 5.187(4)	174.1(1)
		F′ (GSZ)	a_F = 5.584(1)	139.6(2)
11	$Th_{0.5}Zr_{0.5}O_2$	F (ThO_2)	a_F = 5.584(1)	174.1(1)
		M (ZrO_2)	a_M = 5.142,b_M = 5.200 c_M = 5.311, β_M = 99.205°	140.1(3)

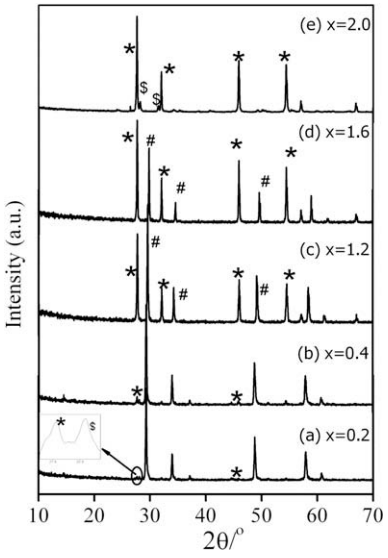

Fig. 2. XRD patterns of (a) x = 0.2, (b) x = 0.4, (c) x = 1.2, (d) x = 1.6, and (e) x = 2.0. Inset of Fig. 2(a) shows the presence of ThO_2 and unreacted m-ZrO_2 (* represents ThO_2, # represents GSZ, $ represents unreacted monoclinic ZrO_2.)

ThO_2 can act as host lattices for $GdO_{1.5}$ but surprisingly, $GdO_{1.5}$ gets dissolved in zirconia only, not in thoria as seen by unchanged lattice parameter of thoria through out the compositions (Table 1). The peak intensity of GSZ phase is higher in $Gd_{0.8}Th_{1.2}Zr_2O_{7.6}$ compared to that in $Gd_{0.4}Th_{1.6}Zr_2O_{7.8}$ which is obviously due to higher GSZ content in the former composition than the later one. The end member of this series i.e. $Th_2Zr_2O_8$ is found to be a mixture of monoclinic ZrO_2 and fluorite ThO_2 which could be due to the considerable ionic size difference between Zr^{4+} and Th^{4+}. This is in agreement with earlier studies [33].

Fig. 3 shows a scanning electron micrographs of $Gd_{2-x}Th_xZr_2O_{7+x/2}$ (x = 0.0, 0.2). From the micrographs it is clear that the pellets are porous. In the present study, the samples were prepared by standard ceramic sintering route, which does not result into highly sintered pellets. Probably, since the composition $Gd_2Zr_2O_7$ is single phasic (Fig. 3(a)) so the nature of the grains are of similar kind. As per XRD analysis, the secondary phase in $Gd_{1.8}Th_{0.2}Zr_2O_{7.1}$ is smaller in quantity so probably the presence of bright phase is difficult to observe in SEM image (Fig. 3(b)).

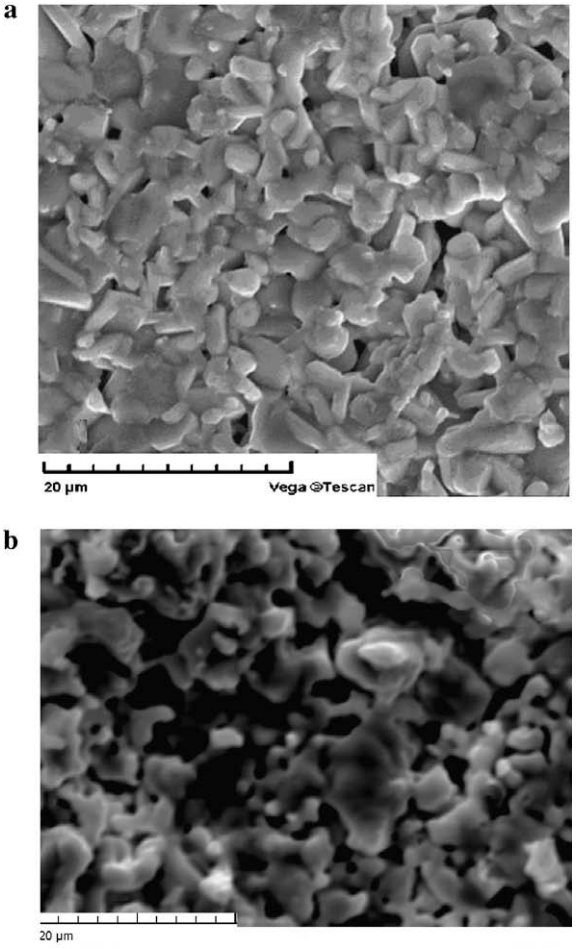

Fig. 3. Scanning electron micrograph of (a) $Gd_2Zr_2O_7$, and (b) $Gd_{1.8}Th_{0.2}Zr_2O_{7.1}$.

Raman spectroscopic investigations were also carried out on all these samples (Fig. 4). Pure $Gd_2Zr_2O_7$ which crystallizes in the defect pyrochlore structure with space group $Fd\bar{3}m$ has six Raman active modes which are $A_{1g} + E_g + 4F_{2g}$ [34]. However, the Raman spectra of the defect fluorites ($A_{0.5}B_{0.5}O_{1.75}$) has a single broad band as the seven oxygen ions in the fluorite structure are randomly distributed over the eight anion sites which gives rise to disorder.

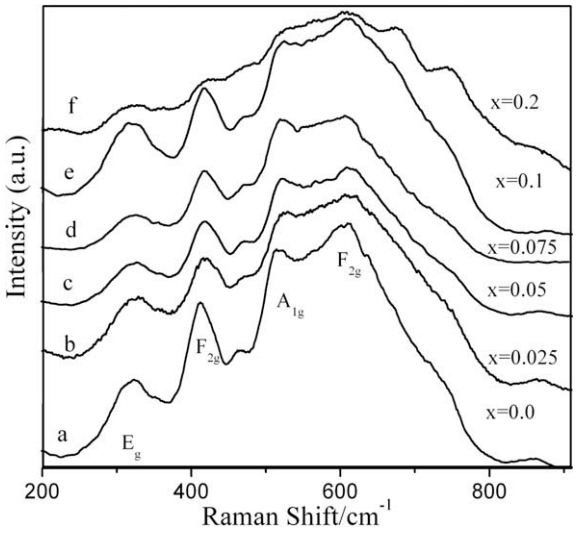

Fig. 4. Raman spectra of $Gd_{2-x}Th_xZr_2O_7$, (a) $x = 0.0$, (b) $x = 0.025$, (c) $x = 0.05$, (d) $x = 0.075$, (e) $x = 0.1$, and (f) $x = 0.2$.

Due to this disorder the Raman spectrum is reduced to a broad continuum of density of states. Only four Raman modes of the $Gd_2Zr_2O_7$ pyrochlore were observed at 321, 412, 518, and 608 cm^{-1} respectively. Zhang et al. [35] also found broad continuum Raman peak for $Gd_2Zr_2O_7$ which support our findings. They are in quite good agreement with the values reported in the literature [36]. A very broad band at ~743 cm^{-1} has been observed. This has been found in several other pyrochlores and has been assigned to the distortion of the octahedra or to the combination band [34] or it could be due to the forbidden modes as assigned by Oueslati et al. [37]. This broadening cannot be attributed to the nano nature of the samples as the diffraction peaks of this phase are quite sharp and indicate that the size of the particles is of the order of a few microns. The Raman spectra of gadolinium zirconate looks similar to that of $Dy_2Hf_2O_7$ indicating that it has an inherent disorder [38]. Assignments of the peaks have been done based on lattice dynamical calculation in different systems [39,40]. The Raman-active band at 321 cm^{-1} is identified as the E_g mode, whereas the other two vibrational frequencies at 412 and 608 cm^{-1} may be assigned to two of the four F_{2g} modes. Following the work of previous researchers [41–43] the Raman band at 518 cm^{-1}, has been assigned as the A_{1g} mode. Two more peaks at around 500 and 845 cm^{-1} are absent in Raman spectra of $Gd_2Zr_2O_7$ which were present in the ordered pyrochlore [30]. The Raman peak at 460 cm^{-1} has been assigned to unreacted zirconia [44] although no peaks corresponding to zirconia has been found in XRD patterns. This may be due to very low concentration of unreacted zirconia in the sample and laboratory X-ray source could not detect it. Earlier also it has been found in few cases where the secondary phase could not be detected by lab-XRD [38,45]. However, synchrotron source could detect the impurity phase in the previous experiments.

Deviation from stoichiometry increases the rate of imperfection and hence less-resolved Raman bands are obtained. We can clearly see that as the concentration of ThO_2 increases i.e. there is a deviation from ideal stoichiometry the width of the Raman modes increases. The plausible reason could be that with the introduction of ThO_2 in the system, the lattice disorder increases due to filling of vacancies by excess oxygen atoms, incorporated due to charge balance. It has been argued that even in an ordered compound there is considerable disorder in the form of vacancy, defects and presence of 'foreign' atoms/ions (for alloys and mixed systems) which breaks down the translational periodicity of the lattice and hence relaxes the $k \approx 0$ selection rule. As the concentration of thoria increases beyond $x = 0.1$ we can see that a new Raman mode is observed at 672 cm^{-1}. We have assigned this mode to $Zr–O_7$ species in accordance with Glerup et al. [46]. The presence of this mode indicates that the pyrochlore structure is becoming disordered as the presence of seven coordination number clearly corresponds to disordered pyrochlores. In $x = 0.1$ and 0.2, the peak at 460 cm^{-1} corresponds to F_{2g} peak of ThO_2 and unreacted ZrO_2 which again supports the presence of secondary phase (ThO_2) in the samples.

4. Conclusions

In this study, a series of samples having nominal compositions $Gd_{2-x}Th_xZr_2O_{7+x/2}$ were prepared by a ceramic sintering route and characterized by various techniques. From XRD and Raman spectroscopic analysis it has been found that 7.5 mol% ThO_2 gets dissolved in $Gd_2Zr_2O_7$ pyrochlore without disturbing the parent structure. The excess oxygen incorporated in the lattice causes lattice expansion though the dopant ion (Th^{4+}) is having very similar ionic radii with that of the host ion (Gd^{3+}). As ThO_2 content in the compositions becomes $\geqslant 0.1$, the secondary phase comes out from the system. In this study we have shown that $GdO_{1.5}$ can stabilize cubic zirconia if it present in sufficient amount. One more concluding remark is that thoria does not dissolve gadolinia if zirconia is present in the compositions which indicates that zirconia has a higher affinity for gadolinia in comparison to thoria. Moreover, pyrochlore is immune to devitrification and can immobilize radwaste for long periods in appropriate geological–geochemical environment. This data might be useful to study the solubility of other minor actinides in $Gd_2Zr_2O_7$.

Acknowledgements

Authors are thankful to Ms S. Sohni for helping in sample preparation and Dr Debnath, TPPED, BARC for SEM studies.

References

[1] H. Kleycamp, J. Nucl. Mater. 275 (1999) 1.
[2] G.J. McCarthy, W.B. White, R. Roy, B.E. Scheetz, S. Komarzeni, D.S. Smith, D.M. Roy, Nature 273 (1978) 216.
[3] A.E. Ringwood, S.E. Kesson, N.G. Ware, W. Hibberson, A. Major, Nature 278 (1979) 219.
[4] S.J. Patwe, A.K. Tyagi, Ceram. Int. 32 (2006) 545.
[5] J.M. Paratte, R. Chawla, Ann. Nucl. Energy 22 (1995) 471.
[6] M. Burghartz, H. Matzke, C. Leger, V. Vambenepe, M. Roma, J. Alloys Compd. 271 (1998) 544.
[7] K. Ferguson, Trans. Am. Nucl. Soc. 75 (1996) 75.
[8] I. Hayakawa, H. Kamizono, J. Nucl. Mater. 202 (1993) 163.
[9] K.E. Sickafus, L. Minervini, R.W. Grimes, J.A. Valdez, M. Ishimaru, F. Li, K.J. McClellan, T. Hartmann, Science 289 (2000) 748.
[10] R.C. Ewing, W.J. Weber, J. Lian, J. Appl. Phys. 95 (2004) 5949.
[11] S. Lutique, D. Staicu, R.J.M. Konings, V.V. Rondinella, J. Somers, T. Wiss, J. Nucl. Mater. 319 (2003) 59.
[12] M.A. Subramanian, G. Aravamudan, G.V. Subba Rao, Prog. Solid State Chem. 15 (1983) 55.
[13] F. Jona, G. Shirane, R. Pepinsky, Phys. Rev. 98 (1955) 903.
[14] H. Nyman, S. Andersson, B.G. Hyde, M. O'Keeffe, J. Solid State Chem. 26 (1978) 123.
[15] S.J. Yates, P. Xu, J. Wang, J.S. Tulenko, J.C. Nino, J. Nucl. Mater. 362 (2007) 336.
[16] S. Lutique, R.J.M. Konings, V.V. Rondinella, J. Somers, T. Wiss, J. Alloys Compd. 352 (2003) 1.
[17] H.H. Kung, J.S. Jarrett, A.W. Sleight, A. Ferretti, J. Appl. Phys. 48 (1977) 2463.
[18] D.P. Cann, C.A. Randall, T.R. Shrout, Solid State Commun. 7 (1996) 529.
[19] B.P. Mandal, S.K. Deshpande, A.K. Tyagi, J. Mater. Res. 23 (2008) 911.
[20] M.J.D. Ruston, R.W. Grimes, C.R. Stanek, S. Owens, J. Mater. Res. 19 (2004) 1603.
[21] C. Nastren, R. Jardin, J. Somers, M. Walter, B. Brendebach, J. Solid State Chem., doi: 10.1016/J.jssc.2008.09.017.
[22] J. Lian, F.X. Zhang, M.T. Peters, L.M. Wang, R.C. Ewing, J. Nucl. Mater. 362 (2007) 438.
[23] J. Lian, X.T. Zu, K.V.G. Kutty, J. Chen, L.M. Wang, R.C. Ewing, Phys. Rev. B 66 (2002) 054108.

[24] B.P. Mandal, A.K. Tyagi, J. Alloys Compd. 437 (2007) 260.
[25] R.J.M. Konings, K. Bakker, J.G. Boshoven, H. Hein, M.E. Huntellar, R.R. van der Laan, J. Nucl. Mater. 274 (1999) 84.
[26] J. Lian, L.M. Wang, R.G. Haire, K.B. Helean, R.C. Ewing, Nucl. Instrum. Meth. Phys. Res. B 218 (2004) 236.
[27] B.P. Mandal, A.K. Tyagi, Mater. Sci. Eng. B 136 (2007) 46.
[28] S. Kramer, M. Spears, H.L. Tuller, Solid State Ionics 72 (1994) 59.
[29] R.D. Shannon, Acta Cryst. A32 (1976) 751.
[30] Z. Qu, C. Wan, W. Pan, Chem. Mater., doi: 10.1021/cm071615z.
[31] V. Grover, A.K. Tyagi, J. Solid State Chem. 177 (2004) 4197.
[32] V. Grover, A.K. Tyagi, J. Am. Ceram. Soc. 89 (2006) 2917.
[33] V. Grover, A.K. Tyagi, J. Nucl. Mater. 305 (2002) 83.
[34] M.T. Vandenborre, E. Husson, J.P. Chatry, D. Michel, J. Raman Spectrosc. 14 (1983) 63.
[35] F.X. Zhang, J. Lian, U. Becker, R.C. Ewing, Jingzhu Hu, S.K. Saxena, Phys. Rev. B 76 (2007) 214104.
[36] B.P. Mandal, A. Banerji, V. Sathe, S.K. Deb, A.K. Tyagi, J. Solid State Chem. 180 (2007) 2643.
[37] M. Oueslati, M. Balkanski, P.K. Moon, H.L. Tuller, Mater. Res. Soc. Symp. Proc. 135 (1989) 199.
[38] B.P. Mandal, N. Garg, S.M. Sharma, A.K. Tyagi, Solid State Chem. 179 (2006) 1999.
[39] S. Brown, H.C. Gupta, J.A. Alonso, M.J. Martinez-Lope, J. Raman Spectrosc. 34 (2003) 240.
[40] H.C. Gupta, S. Brown, J. Phys. Chem. Sol. 64 (2003) 2205.
[41] B.E. Scheetz, W.B. White, J. Am. Ceram. Soc. 62 (1979) 468.
[42] N.J. Hess, B.D. Begg, S.D. Conradson, D.E. McCready, P.L. Gassman, W.J. Weber, J. Phys. Chem. B 106 (2002) 4663.
[43] F.X. Zhang, B. Manoun, S.K. Saxena, C.S. Zha, Appl. Phys. Lett. 86 (2005) 181906.
[44] Florence Boulc'h, Elisabeth Djurado, Solid State Ionics 157 (2003) 335.
[45] N. Garg, K.K. Pandey, C. Murli, K.V. Shanavas, B.P. Mandal, A.K. Tyagi, S.M. Sharma, Phys. Rev. B 77 (2008) 214105.
[46] M. Glerup, O.F. Nielsen, F.W. Poulsen, J. Solid State Chem. 160 (2001) 25.